JOURNAL OF Applied Polymer SCIENCE

Special Issue: Bio-based Packaging

Guest Editors: José M. Lagarón, Amparo López-Rubio, and María José Fabra
Institute of Agrochemistry and Food Technology of the Spanish Council for Scientific Research

EDITORIAL

REVIEWS

RESEARCH ARTICLES

JOURNAL OF Applied Polymer SCIENCE

Special Issue: Bio-based Packaging

Guest Editors: José M. Lagarón, Amparo López-Rubio, and María José Fabra
Institute of Agrochemistry and Food Technology of the Spanish Council for Scientific Research

Impact of fermentation residues on the thermal, structural, and rheological properties of polyhydroxy(butyrate-*co*-valerate) produced from cheese whey and olive oil mill wastewater
L. Hilliou, D. Machado, C. S. S. Oliveira, A. R. Gouveia, M. A. M. Reis, S. Campanari, M. Villano and M. Majone, *J. Appl. Polym. Sci.* 2015, DOI: 10.1002/app.42818

Synergistic effect of lactic acid oligomers and laminar graphene sheets on the barrier properties of polylactide nanocomposites obtained by the in situ polymerization pre-incorporation method
J. Ambrosio-Martín, A. López-Rubio, M. J. Fabra, M. A. López-Manchado, A. Sorrentino, G. Gorrasi and J. M. Lagarón, *J. Appl. Polym. Sci.* 2015, DOI: 10.1002/app.42661

Antibacterial poly(lactic acid) (PLA) films grafted with electrospun PLA/allyl isothiocyanate fibers for food packaging
H. H. Kara, F. Xiao, M. Sarker, T. Z. Jin, A. M. M. Sousa, C.-K. Liu, P. M. Tomasula and L. Liu, *J. Appl. Polym. Sci.* 2015, DOI: 10.1002/app.42475

Poly(L-lactide)/ZnO nanocomposites as efficient UV-shielding coatings for packaging applications
E. Lizundia, L. Ruiz-Rubio, J. L. Vilas and L. M. León, *J. Appl. Polym. Sci.* 2015, DOI: 10.1002/app.42426

Effect of electron beam irradiation on the properties of polylactic acid/montmorillonite nanocomposites for food packaging applications
M. Salvatore, A. Marra, D. Duraccio, S. Shayanfar, S. D. Pillai, S. Cimmino and C. Silvestre, *J. Appl. Polym. Sci.* 2015, DOI: 10.1002/app.42219

Preparation and characterization of linear and star-shaped poly L-lactide blends
M. B. Khajeheian and A. Rosling, *J. Appl. Polym. Sci.* 2015, DOI: 10.1002/app.42231

Mechanical properties of biodegradable polylactide/poly(ether-block-amide)/thermoplastic starch blends: Effect of the crosslinking of starch
L. Zhou, G. Zhao and W. Jiang, *J. Appl. Polym. Sci.* 2015, DOI: 10.1002/app.42297

Interaction and quantification of thymol in active PLA-based materials containing natural fibers
I. S. M. A. Tawakkal, M. J. Cran and S. W. Bigger, *J. Appl. Polym. Sci.* 2015, DOI: 10.1002/app.42160

Graphene-modified poly(lactic acid) for packaging: Material formulation, processing, and performance
M. Barletta, M. Puopolo, V. Tagliaferri and S. Vesco, *J. Appl. Polym. Sci.* 2015, DOI: 10.1002/app.42252

Edible films based on chia flour: Development and characterization
M. Dick, C. H. Pagno, T. M. H. Costa, A. Gomaa, M. Subirade, A. De O. Rios and S. H. Flóres, *J. Appl. Polym. Sci.* 2015, DOI: 10.1002/app.42455

Influence of citric acid on the properties and stability of starch-polycaprolactone based films
R. Ortega-Toro, S. Collazo-Bigliardi, P. Talens and A. Chiralt, *J. Appl. Polym. Sci.* 2015, DOI: 10.1002/app.42220

Bionanocomposites based on polysaccharides and fibrous clays for packaging applications
A. C. S. Alcântara, M. Darder, P. Aranda, A. Ayral and E. Ruiz-Hitzky, *J. Appl. Polym. Sci.* 2015, DOI: 10.1002/app.42362

Hybrid carrageenan-based formulations for edible film preparation: Benchmarking with kappa carrageenan
F. D. S. Larotonda, M. D. Torres, M. P. Gonçalves, A. M. Sereno and L. Hilliou, *J. Appl. Polym. Sci.* 2015, DOI: 10.1002/app.42263

JOURNAL OF Applied Polymer SCIENCE

Special Issue: Bio-based Packaging

Guest Editors: José M. Lagarón, Amparo López-Rubio, and María José Fabra
Institute of Agrochemistry and Food Technology of the Spanish Council for Scientific Research

Structural and mechanical properties of clay nanocomposite foams based on cellulose for the food packaging industry
S. Ahmadzadeh, J. Keramat, A. Nasirpour, N. Hamdami, T. Behzad, L. Aranda, M. Vilasi and S. Desobry, *J. Appl. Polym. Sci.* 2015, DOI: 10.1002/app.42079

Mechanically strong nanocomposite films based on highly filled carboxymethyl cellulose with graphene oxide
M. El Achaby, N. El Miri, A. Snik, M. Zahouily, K. Abdelouahdi, A. Fihri, A. Barakat and A. Solhy, *J. Appl. Polym. Sci.* 2015, DOI: 10.1002/app.42356

Production and characterization of microfibrillated cellulose-reinforced thermoplastic starch composites
L. Lendvai, J. Karger-Kocsis, Á. Kmetty and S. X. Drakopoulos, *J. Appl. Polym. Sci.* 2015, DOI: 10.1002/app.42397

Development of bioplastics based on agricultural side-stream products: Film extrusion of *Crambe abyssinica*/wheat gluten blends for packaging purposes
H. Rasel, T. Johansson, M. Gällstedt, W. Newson, E. Johansson and M. Hedenqvist, *J. Appl. Polym. Sci.* 2015, DOI: 10.1002/app.42442

Influence of plasticizers on the mechanical and barrier properties of cast biopolymer films
V. Jost and C. Stramm, *J. Appl. Polym. Sci.* 2015, DOI: 10.1002/app.42513

The effect of oxidized ferulic acid on physicochemical properties of bitter vetch (*Vicia ervilia*) protein-based films
A. Arabestani, M. Kadivar, M. Shahedi, S. A. H. Goli and R. Porta, *J. Appl. Polym. Sci.* 2015, DOI: 10.1002/app.42894

Effect of hydrochloric acid on the properties of biodegradable packaging materials of carboxymethylcellulose/poly(vinyl alcohol) blends
M. D. H. Rashid, M. D. S. Rahaman, S. E. Kabir and M. A. Khan, *J. Appl. Polym. Sci.* 2015, DOI: 10.1002/app.42870

Journal of Applied Polymer Science

Mechanically strong nanocomposite films based on highly filled carboxymethyl cellulose with graphene oxide

Mounir El Achaby,[1] Nassima El Miri,[2,3] Asmae Snik,[2] Mohamed Zahouily,[2,3] Karima Abdelouahdi,[4] Aziz Fihri,[3] Abdellatif Barakat,[5] Abderrahim Solhy[1]

[1]Center For Advanced Materials, Université Mohammed VI Polytechnique, Lot 660-Hay Moulay Rachid, 43150 Ben Guerir, Morocco
[2]Laboratoire de Matériaux, Catalyse & Valorisation des Ressources Naturelles (LMaCaVa, URAC 24) FST Mohammedia, Université Hassan II Casablanca Quartier des Hôpitaux, Morocco
[3]MAScIR Foundation, Rabat Design, Rue Mohamed El Jazouli, Madinat Al Irfane 10100 Rabat, Morocco
[4]Division UATRS, Centre National pour la Recherche Scientifique et Technique (CNRST), Angle Allal Fassi/FAR, B.P. 8027, Hay Riad, 10000 Rabat, Morocco
[5]INRA, UMR 1208 Ingénierie des Agropolymères et Technologies Emergentes (IATE) 2, place Pierre Viala - 34060 Montpellier Cedex 1, France
Correspondence to: M. El Achaby (E-mail: mounir.elachaby@um6p.ma) and A. Solhy (E-mail: abderrahim.solhy@um6p.ma)

ABSTRACT: Biopolymer nanocomposite films were prepared by adding exfoliated graphene oxide nanosheets (GOn) into carboxymethyl cellulose (CMC) at low and high GOn loadings (0.4–7 wt %). As firstly evidenced by viscosity of film-forming solutions, microscopic observations and infrared spectroscopy measurements, it was found that the GOn form a three-dimensional network throughout strong interfacial interactions with CMC, confirming that the GOn were well dispersed within the CMC, even at high GOn content, owing to the presence of several multifunctional groups on both phases which ensured the high compatibility between them. The topography of as prepared films was characterized by atomic force microscopy measurements showing that the films have a smooth surface with a very low average roughness for all range of GOn contents. Furthermore, the thermal stability, glass transition temperature, and tensile properties of nanocomposite films were gradually increased with increasing of GOn contents. By adding 7 wt % GOn, 18% increases of thermal stability, 17% of glass transition temperature, 623% of Young's modulus, and 268% of tensile strength were achieved. This work produced structured CMC-based nanocomposite films containing low and high loadings of well-dispersed GOn. The high performances of these films can be expected to have potential in biomaterials or packaging materials applications. © 2015 Wiley Periodicals, Inc. J. Appl. Polym. Sci. **2016**, *133*, 42356.

KEYWORDS: biopolymers & renewable polymers; composites; films; interfaces; mechanical properties; surfaces

Received 11 December 2014; accepted 13 April 2015
DOI: 10.1002/app.42356

INTRODUCTION

The plastic industry has made significant progress toward sustainable development and environment management.[1,2] The attempt concerns the replacement of polymers derived from petroleum with superior biodegradable polymers.[3] In this sense, biopolymers have attracted special attention to be considered as potential replacement for the conventional plastic materials. Nevertheless, it is worth mentioning here that additional developments and investigations are required to improve their properties to position them as essential materials able to compete with fossil derivative products. For instance, biopolymer based nanocomposites technology consisting of fabricating biopolymer matrix reinforced by appropriate nanofillers can be considered as reliable approach to enhance the basic properties of the neat biopolymer.[1]

Recently the incorporation of a large variety of nanofillers, such as graphene,[1,2,4] carbon nanotubes and nanofibers,[5,6] carbon black,[7] nanodiamond,[8] nanoclay,[9] and cellulose nanocrystals,[3,10] in the biopolymers has been observed to lead to significant enhancements in their mechanical, thermal, rheological, and gas barrier properties.

The discovery of graphene, which is a one-atom-thick planar layer of carbon atoms that are self-assembled in a honeycomb-type two-dimensional (2D) lattice,[11] has attracted substantial interest due to its outstanding properties, of which have already been exploited as nanofillers into a matrix to form nanocomposites.[12–15] However, graphene is incompatible with most organic polymers; thus, its oxygenated counterpart like graphene oxide, has been used as compatible nanomaterial.[1] Graphene oxide is a

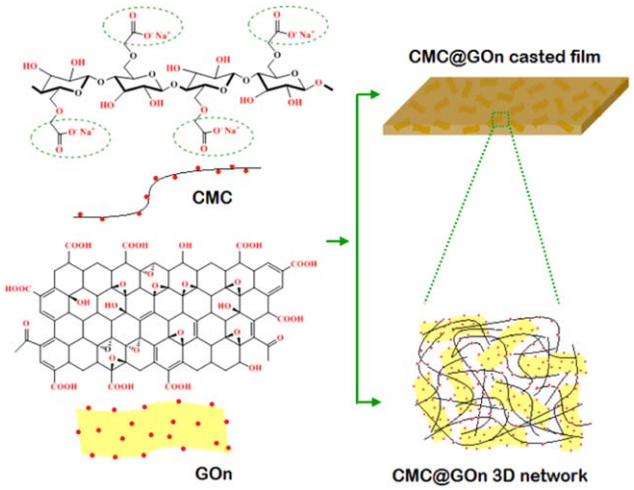

Figure 1. Schematic representation of the structures of based products (CMC and GOn) and their well dispersed bio-nanocomposite cast film. [Color figure can be viewed in the online issue, which is available at wileyonlinelibrary.com.]

single layer of graphite oxide obtained through a process of oxidation/exfoliation of natural graphite.[16] Graphene oxide nanosheets (GOn) are essentially graphene nanosheets in which oxygen-containing functional groups are thought to be present in the form of carboxyl, hydroxyl, and epoxy groups.[16–19] The high properties and benefits of GOn have generated an active area of research, where many investigations have shown potential applications in various technological fields.[20–24] Because of the very hydrophilic character of graphite oxide, an aqueous colloidal suspension of GOn can easily be obtained by complete exfoliation of bulk graphite oxide via simple sonication in water.[16–19]

In the field of biopolymer nanocomposites, two things must be achieved to carry over the exceptional properties of the nanofiller in a biopolymer matrix. The first is the need for good dispersion and distribution of the nanofiller in the matrix, while the second is the need for a high degree of interaction between the nanofiller and the macromolecular chains of biopolymer. These mechanisms can be ensured by the high compatibility between the surface of the nanofiller and the macromolecular chains of the polymer.[1] In this context, the functional groups of GOn can serve as sites of chemical anchorage, improving the dispersion and distribution of nanosheets and generating high interfacial interactions with the functional groups of water soluble biopolymer matrices, such as the carboxymethyl cellulose (CMC) biopolymer, and thus take advantage of the outstanding properties of graphene materials.[1]

Recent prominent studies have explored GOn's potential to make functional biopolymer based nanocomposites using several matrices such as chitosan,[1,2,25] CMC,[26,27] starch,[1,28] alginate,[29] polylactic acid,[30,31] and gelatin.[32] These biopolymer based nanocomposites showed high improvement in thermal, mechanical, electrical, and bioactivity properties at a very low GOn loading. However, it has been reported that the GOn start to aggregate when their loading level became higher than a critical content, with a maximum of 3 wt %.[33–35] This is mainly attributed to the inadequate compatibility between the sheet and polymer chains, leading to the sheet–sheet interaction.

Thus, with an aim to use biopolymers as materials that can be competitive with the fossil derivatives, the research on GOn filled biopolymer nanocomposites has gained considerable momentum. CMC, the sodium salt of the carboxymethyl ether of cellulose, is an anionic polymer from cellulose, monochloroacetic acid, and sodium hydroxide.[36] This biopolymer has diverse and interesting properties, including biocompatibility, nontoxicity, biodegradability, and film-forming ability.[37] These properties make CMC one of the most important cellulose derivatives. CMC is widely used in various technological applications.[38–43] Biodegradable films made of this material do not pose a threat to the environment, and has a relatively low cost and is non-toxic. However, the disadvantages of this film include poor mechanical properties and a strong hydrophilic nature.[44]

Recently, some researchers studied CMC nanocomposites filled by GOn. Wang *et al.* studied the non-linear optical properties of GOn filled CMC nanocomposite films. They revealed that GOn are specific nanomaterials to enhance the optical properties of CMC.[45] The morphological, thermal, and tensile properties of GOn filled CMC nanocomposites were studied by Layek *et al.* by varying the GOn weight fractions from 0.25 to 1 wt %. They found that the successful nanocomposite formation is facilitated by hydrogen bonding interaction between GOn and CMC.[26] From their results, the selected properties are gradually improved with increasing of GOn content. For example, the storage modulus, Young's modulus, and tensile strength were increased by 174, 154 and 188%, respectively, when 1 wt % GOn is added. In the same way, Yadav *et al.* developed also GOn filled CMC nanocomposite at different GOn contents (0.5–1 wt %). A maximum increase of Young's modulus and tensile strength of 148 and 67% has been observed in the nanocomposite containing 1 wt % GOn.[27] It is very interesting to develop such nanocomposite materials at high GOn content, in order to verify the structure and the properties of CMC based nanocomposites containing high amounts of GOn and to propose a biocompatible nanocomposite material with very high improvement of its properties, which can be potential for biomaterials or packaging materials applications.

In this study, low and high GOn contents and CMC biopolymer were mixed to produce structured CMC-based nanocomposite films, where GOn worked as the 2D cross-linker due to its multifunctional groups on both sides and edges. CMC and GOn have hydrophilic nature and both have oxygen-containing groups. Therefore, these two components can easily be mixed in water. Thus, the aim of this study is to prepare biocompatible and mechanically strong nanocomposite films by dispersing GOn in CMC biopolymer using the solution casting method, as shown in Figure 1. The effect of low and high GOn fractions (0.4–7 wt %) on the morphology, structural, thermal, and mechanical properties of CMC-based nanocomposite films has been evaluated and discussed in this report.

EXPERIMENTAL

Materials and Methods

Exfoliated GOn were prepared via chemical oxidation of natural graphite (≤20 μm, 99.99%, Sigma-Aldrich) followed by

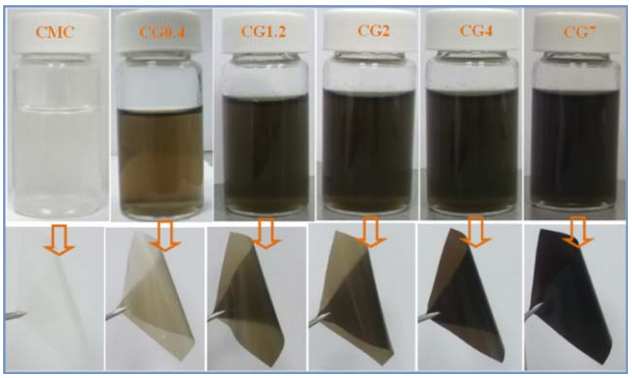

Figure 2. Digital images of neat CMC and CMC@GOn film-forming solutions and the corresponding isolated solid films (≈70 μm) with various GOn contents. [Color figure can be viewed in the online issue, which is available at wileyonlinelibrary.com.]

sonication assisted water-phase exfoliation in accordance to our previous works.[14,15,46,47] In order to prepare 0.4, 1.2, 2, 4, and 7 wt % GOn filled CMC nanocomposite films, 0.016/0.056/0.08/0.16/0.28 g of graphite oxide powder were dispersed into 250 mL of deionized water and sonicated for 1 hour to obtain homogeneous and stable exfoliated GOn suspensions. Then, 3.984/3.944/3.920/3.840/3.720 g of high molecular weight CMC sodium salt powder (CAS 9004-32-4, Alfa easer) were slowly added to the GOn dispersions, respectively, and stirred for 4 hours. The obtained CMC@GOn homogeneous mixtures (Figure 2) were poured onto PET sheets and kept in air to slow evaporation of water. Then, the films were peeled from the sheets and kept in vacuum oven at 60°C for 12 hours, for the complete elimination of physisorbed water. Neat CMC film without addition of GOn was prepared by the same procedure. The samples are referenced as CMC, CG0.4, CG1.2, CG2, CG4, and CG7, respectively (Figure 2). The number in each code name indicates the weight fraction of GOn in nanocomposites.

Characterization Techniques

Atomic force microscopy (AFM) measurements were carried out using a Veeco Dimension ICON. The tapping mode was used to capture height sensor images at a scan rate of 1.5 Hz. The samples used for AFM characterizations were deposited from aqueous GOn dispersion on mica sheets and allowing the solvent to dry in air. The steady shear viscosity measurements were performed at 20°C, using a rotational Physica MCR500 rheometer equipped with concentric cylinder geometry (CC27). The temperature was regulated by a Paar Physica circulating bath and a controlled peltier system (TEZ 150P-C). Fourier transform infrared spectroscopy (FTIR) was performed on an ABB Bomem FTLA 2000 spectrometer equipped with a Golden Gate single reflection ATR accessory. The UV–Vis spectroscopy analysis was carried out using a PerkinElmer LAMBDA 1050 UV/Vis/NIR Spectrophotometer. Films were mounted with their surface perpendicular to the incident light and referenced to air. Transmission electron microscope (TEM) was performed by using a FEI Tecnai G2 microscope operated at an accelerated voltage of 120 kV. Nanocomposite thin films of CMC@GOn were deposited from the homogenous mixture on the carbon coated copper grid and left to dry for 12 hours at 70°C. Thermogravimetric analyses (TGA) were conducted under nitrogen gas, using a TGA-Q500 (TA Instruments) apparatus with 10°C/min ramp between 25°C and 600°C. Differential scanning calorimetry (DSC) was carried out under nitrogen gas with 10°C/min heating rate from −20 to 200°C using a DSC-Q100 (TA Instrument); and the sample mass was approximately 10 mg for each sample. Tensile tests were performed using an Instron 8821S tensiometer. The tensile specimens were cut in rectangular shapes with dimensions of 80 mm in length and 10 mm in width. The gauge length was fixed at 25 mm and the speed of the moving clamp was 10 mm/min. All tests were carried out on a minimum of five samples and the reported results are average values.

RESULTS AND DISCUSSION

As previously stated, CMC and GOn both contain hydroxyl and carboxyl groups and have hydrophilic character, their mixture in water can easily be achieved in controlled conditions, enabling the formation of a homogeneous and stable mixture in aqueous media. Figure 2 shows the photographs of a neat CMC solution and its mixture with different amounts of GOn. The photographs were recorded at room temperature and 10 days after their preparation, showing high stability and good homogeneity. By casting these mixtures on plastic plates, films with high quality, smooth surfaces, good flexibility and 70-μm thick were produced. Figure 2 shows the isolated films of pure CMC and its nanocomposites with different amounts of GOn. It can be seen that, with the increase of GOn loading, the transparency of CMC@GOn films was reduced, and the films become darker at high GOn loading level (4 and 7 wt %). We noted that the thickness of these films can be controlled by the amount of the solution used for the casting process. Furthermore, it can be simply cut into various desired forms by using a special knife.

AFM Characterization of GOn

Before blending the suspended GOn with CMC biopolymer, the complete exfoliation of GOn was confirmed by AFM observations. Indeed, individual nanosheets were obtained by intense sonication in water of completely oxidized natural graphite.[14,46] During this operation, it was noted that the bulk graphite oxide dispersion gradually transformed into a yellow brown solution during which the graphite oxide powder was transformed into individual nanosheets. It has been reported that the successful oxidation of graphite is crucial for its complete exfoliation into individual GOn.[14,46,47]

The AFM images of the GOn revealed the presence of irregular shaped nanosheets with uniform thickness and different lateral dimensions (Figure 3). As shown from the diameter distribution and the height profiles that were recorded at different locations, the lateral dimensions (diameter) of the obtained sheets ranged from approximately 100 nm to approximately 2–3 μm, while the thickness was observed at 1 nm (Figure 3). We conclude from this analysis that there were no nanosheets thicker or thinner than 1 nm. This observation could be explained by the efficient top–down process of the exfoliation of graphite oxide in to GOn, achieved by the ultrasonic treatment. However, we would also point out that a single sheet of graphene is atomically flat with a

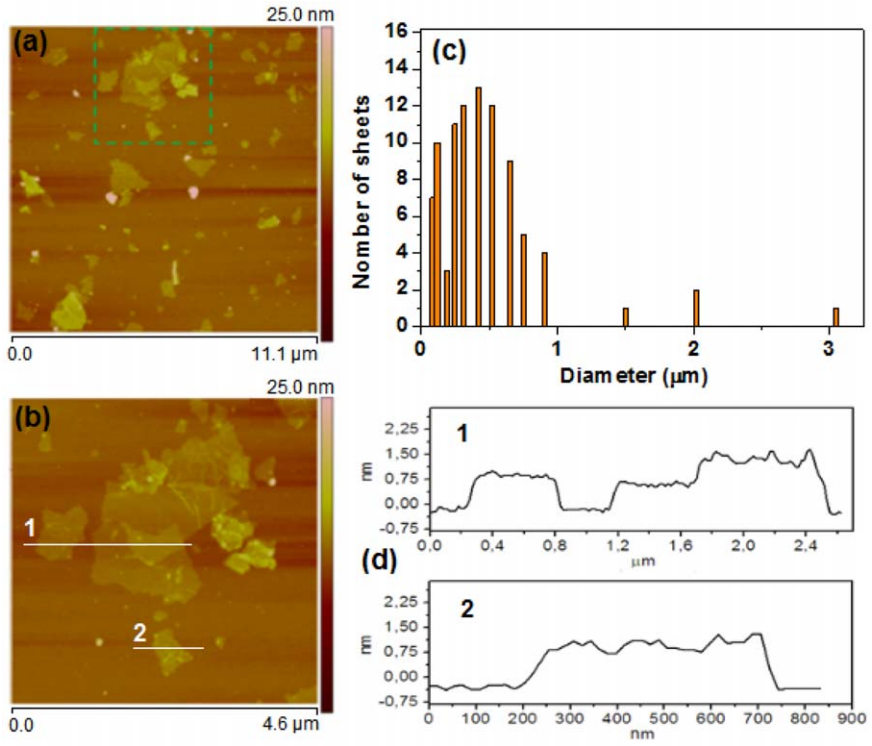

Figure 3. (a) High and (b) low scale AFM images taken in tapping mode, (c) histogram of nanosheet diameter, and (d) two height profiles taken along the indicated lines in image b. [Color figure can be viewed in the online issue, which is available at wileyonlinelibrary.com.]

thickness of 0.34 nm; the sheet of GOn is expected to be thicker due to the presence of oxygen-containing functional groups attached on both sides of the GOn and the displacement of the sp^3-hybridized carbon atoms slightly above and below the original graphene plane.[19,48] In addition, this increased thickness up to 1 nm was owed to the wrinkled and folded structure that creates a space between the sheets and substrate during solvent evaporation. This result is in agreement with our previous work.[46]

Viscosity of Film Forming Solutions

Figure 4(a) illustrates the dependence of the steady shear viscosity (η) on the shear rate (γ) for film forming solutions of neat CMC and its mixtures with GOn, obtained from the steady shear sweep. It should be noted that all solutions were prepared with a 1.6 wt % CMC@GOn concentration (with respect to 100 g of solution). From Figure 4(a), neat CMC solution shows a Newtonian behavior at a low shear rate, which was characterized by the shear rate-independent viscosity. At a higher shear rate, the most pronounced shear-thinning behavior was also observed for the neat CMC solution. This outcome indicates that, as shear rate increases, the intermolecular junctions were disrupted at a rate faster than their rate of reformation, resulting in a decrease of the junction density and hence dropping in viscosity. For nanocomposite solutions, it was observed that the presence of GOn has an effect on the steady state viscosity. At a low shear rate region, the viscosity increases gradually with increasing GOn loadings; this is due to the flow-impeding effect induced by the presence of GOn.[49,50] Furthermore, the presence of GOn restrains the shear flow of the CMC macromolecules because the sheet's lateral size is far larger than that of the chain segment of the biopolymer, resulting in an increase of shear viscosity.[49] Moreover, due to the high affinity between the functional groups of both phases, GOn can form a three-dimensional (3D) network throughout strong interfacial interactions with CMC chains, restricting the mobility of macromolecule chains of CMC (Figure 1). The nanocomposite solutions showed only the shear thinning behavior, in the full shear rate range compared with the neat CMC solution, especially at higher GOn loading levels. This trend has been also observed in our previous work studying ternary bio-nanocomposites based on cellulose nanocrystals filled polyvinyl alcohol/chitosan polymer blend.[50]

In Figure 4(b), the zero shear viscosity (η_0) was estimated by extrapolation along the low shear rate plateau, and the η_0 values determined for all studied solutions were plotted against GOn loadings. The η_0 versus GOn content increased linearly with increasing of GOn content. Consequently, this large viscosity enhancement suggests that the GOn and CMC are perfectly compatible phases via the hydrogen bond interactions, between the functional groups present in both phases.[26] Therefore, a 3D interconnected network is assumed to be formed in CMC based solutions mixed with GOn (Figure 1). Since the special 2D morphology of the GOn as well as its functionalized surface provides a good homogeneous dispersion, leading to a high contact area in the CMC@GOn film-forming solutions. This was mainly the result of strong interactions between the macromolecular chains of polymer and the nanosheets of GOn.

FTIR Characterization of Films

The results obtained regarding the viscosity of film-forming solutions were confirmed by FTIR measurements of the as-

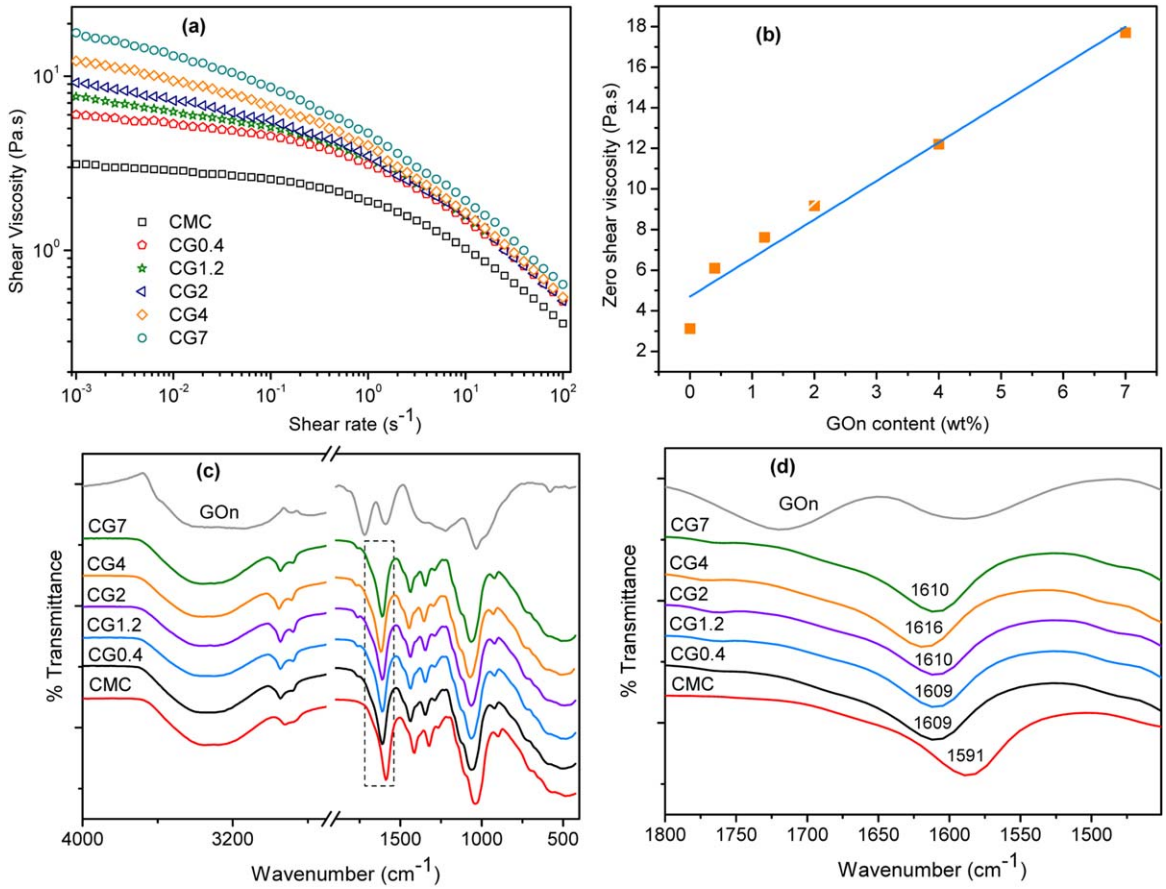

Figure 4. (a) Shear viscosity versus shear rate of film-forming solutions of neat CMC and CMC@GOn, (b) zero shear viscosity as function of GOn content, (c) FTIR spectra of neat CMC and CMC@GOn nanocomposites in the region of 400–4000 cm^{-1}, and (d) in the region of 1450–1800 cm^{-1}. [Color figure can be viewed in the online issue, which is available at wileyonlinelibrary.com.]

prepared solid films. Figure 4(c) shows the FTIR spectra of neat CMC and CMC@GOn films with various GOn contents. For the CMC spectrum, the band at 1042 cm^{-1} is associated to —C—O stretching vibration of ether groups; the bands at 1411 and 1591 cm^{-1} are associated to the asymmetric and symmetric modes of stretching vibration of carboxylate groups, respectively.[26,51] When GOn were added to the CMC, the C═O carbonyl stretch of the carboxylic group observed at 1715 cm^{-1} in the GOn spectrum,[46] was overlapped with that of carboxylate groups of the CMC, indicating that the carboxyl group of GOn showed a strong interaction with the hydroxyl groups present in the CMC. The epoxy groups observed at 1000–1280 cm^{-1} in GOn spectrum,[46,52] can also interact with the hydroxyl groups of CMC biopolymer. Figure 4(d) shows the FTIR spectra in the region of 1450–1800 cm^{-1}. From this figure, it is clear that the peak observed at 1591 cm^{-1} of the carboxyl groups of CMC is shifted to 1609–1616 cm^{-1} as function of GOn content in the nanocomposites; thus confirming that the hydroxyl groups of GOn are strongly interacted with the carboxyl groups of CMC. The strong interaction is observed for CMC containing 4 wt % GOn (CG4 sample), because the highest shift (1616 cm^{-1}) is observed for this sample. Therefore, an interconnected structure is formed in CMC filled by GOn that originated from the strong interactions between the hydroxyl, carboxyl, and epoxy groups of GOn with the hydroxyl and carboxylate groups of CMC biopolymer.[26] These results are in good agreement with those obtained by the other authors for lowly filled CMC nanocomposites with GOn.[26,27]

TEM Characterization of Films

TEM characterizations were employed to investigate the dispersion quality and the morphology of CMC@GOn nanocomposite films. The TEM micrographs of ultrathin films containing 0.4, 2, 4, and 7 wt % of GOn (CG0.4, CG2, CG4, and CG7) are shown in Figure 5. From this figure, a fine dispersion of GOn in the CMC matrix can be clearly observed. In these micrographs, the isolated nanosheets appear as distinct dark lines homogeneously dispersed within the matrix, with a few agglomerates observed at high GOn content (CG7 film) [Figure 5(d)]. One can clearly see that the GOn has been successfully exfoliated and uniformly dispersed throughout the polymeric matrix. Because the presence of oxygen-containing groups on the surface and edge of GOn, the compatibility of GOn with CMC and the quality of dispersion can be significantly improved. The strong interactions between oxygen groups and the CMC chains lead to the homogeneous dispersion of GOn in the CMC matrix, as deduced from the viscosity measurement and FTIR analysis (Figure 4). Therefore, the excellent dispersion of GOn

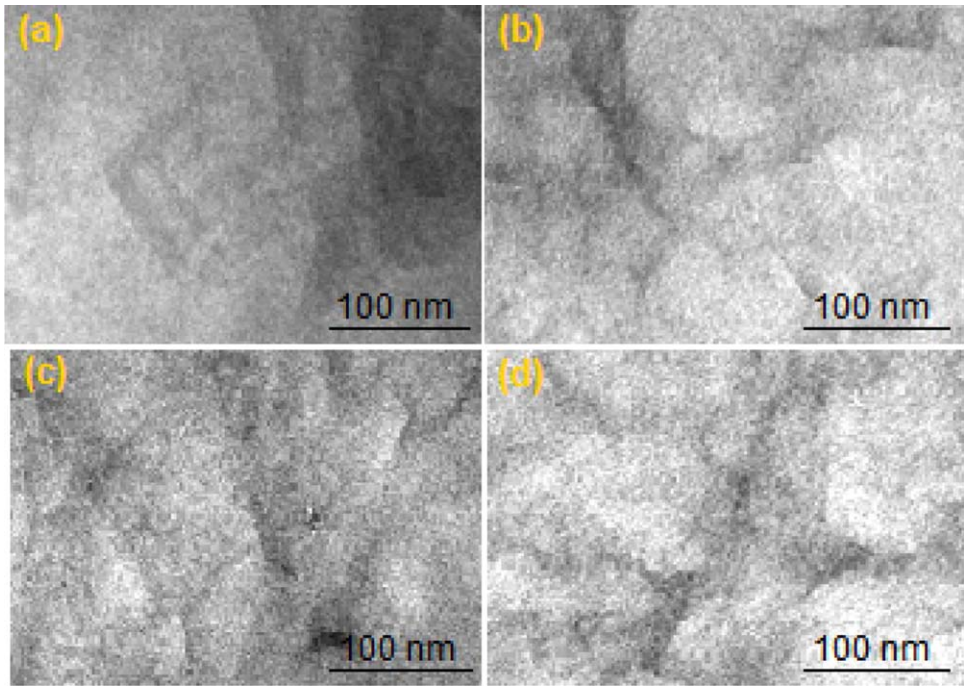

Figure 5. TEM images of CMC@GOn nanocomposite films with (a) CG0.4, (b) CG2, (c) CG4, and (d) CG7 samples. [Color figure can be viewed in the online issue, which is available at wileyonlinelibrary.com.]

in the CMC matrix, at low and high GOn content, is directly correlated with its effectiveness in improving the properties of nanocomposite films.[47]

UV–Vis Spectroscopy of Films

UV–Vis spectroscopy was also used to evaluate the local dispersion characteristics of GOn within the CMC matrix. For that assessment, films of neat CMC and CMC@GOn nanocomposites were characterized and the relative absorbance was recorded and plotted in the UV–Visible region (200–800 nm) [Figure 6(a)]. The scattering intensity at an arbitrarily chosen wavelength (550 nm) was also extracted and plotted against GOn loading [Figure 6(b)]. Evidently, there was not an absorption peak for the CMC polymer, since this polymer is known to be transparent in the UV–visible region. For the CMC films filled by GOn, the absorbance increased gradually with the increase of GOn loadings, especially in the UV region. The absorption spectra of CMC nanocomposite films was dominated by the Raleigh scattering component (the $1/\lambda^4$ tail) from the nanophase dispersed in polymer matrix.[53,54] For each GOn loading, a decrease in absorbance was observed as wavelength increased. The increase in nanosheets loading resulted in the nanocomposite films becoming darker, corresponding to a relative increase in the Rayleigh's tails for the full wavelength range.[46] This can be seen in Figure 6(b) for a wavelength of 550 nm. In general, the lateral size of GOn is more than 100 nm (Figure 3); their presence in nanocomposite films is responsible for scattering and/or absorbing light and to enhance the absorbance level of CMC@GOn films. However, there was not any strong scattering and/or absorbance found, indicating that the GOn were well dispersed at nanoscale within the CMC polymer.[46] The spectrum for the GOn dispersion in water exhibits a maximum at 230 nm and a tiny shoulder at 300 nm, as shown in the inset of Figure 6(a). This can be, respectively, associated to $\pi \rightarrow \pi^*$ transitions of aromatic C═C bonds and n $\rightarrow \pi^*$ transitions of C═O bonds.[46] These peaks were also observed for CMC@GOn films, with few shifts toward low values. This indicated that strong interactions occurred between macromolecular chains of CMC and the functionalized surface of GOn,[26,27] as confirmed by FTIR and viscosity measurements (Figure 4).

Thermal Properties of Films

The DSC was used to investigate the T_g of the CMC@GOn nanocomposite films. It can be observed that the addition of GOn gradually increased the T_g of the CMC matrix, even if at high GOn loading (7 wt %). This observation indicated that the chains' mobility of CMC was more affected when high amounts of GOn were added. As shown in Figure 6(c), the T_g of neat CMC film is about 71.6°C. With the addition of 7 wt % GOn, the maximum increase of T_g is 12°C higher than that of neat CMC biopolymer. The increase in T_g can be ascribed to the effective attachment of CMC to the nanosheets that constrain the segmental motion of the CMC chains by strong hydrogen-bonding interactions, as previously observed from low GOn content filled CMC nanocomposites,[26] where the T_g increased from 67°C for neat CMC to 71°C for CMC nanocomposite containing 1 wt % GOn.

The thermal stability of the nanocomposite films were evaluated with TGA. It should be noted that GOn is a thermally unstable material and shows a significant weight loss (≈50%) at a temperature below 210°C, due to the decomposition of oxygen-containing groups [inset of Figure 6(d)]. In TGA thermograms of CMC and CMC@GOn films, the first weight loss occurred at

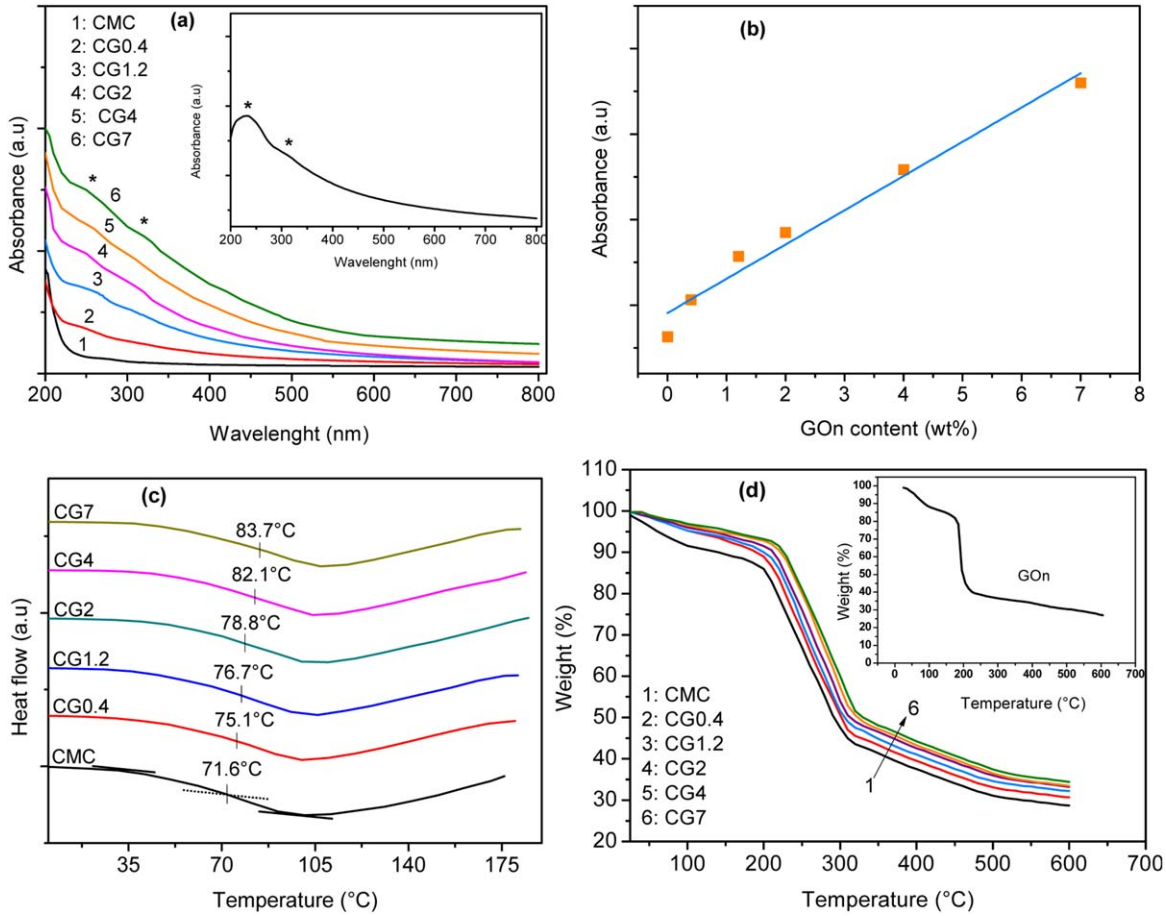

Figure 6. (a) UV–Vis spectra of neat CMC and CMC@GOn films (inset: the UV–Vis absorbance of GOn dispersion) and (b) plot of scattering intensity at 550 nm as function GOn content; (c) DSC and (d) TGA curves of neat CMC and CMC@GOn films (inset: the TGA curve of GOn). [Color figure can be viewed in the online issue, which is available at wileyonlinelibrary.com.]

50°C–100°C and was attributed to the removal of adsorbed water molecules. It should be noted that the amount of absorbed water for neat CMC film was higher than that of CMC@GOn films [Figure 6(d)] suggesting that the GOn nanosheets were well dispersed within the CMC matrix, acting as an interpenetrated network within the CMC matrix, and thus prevented the absorption of water by films when exposed to the moisture.[47] This theory can be supported by the increase of the onset temperature of degradation with the increase of GOn content in the CMC@GOn films. Additionally, in CMC@GOn nanocomposite films, the major mass loss (≈50%) of GOn occurring at around 210 °C was disappeared, suggesting a good interaction between the oxygen functional groups of GOn and the macromolecular chains of CMC polymer This leads in a mobility suppression of the polymer segments at the interfaces between CMC and GOn surface, improvement in turn the thermal stability of CMC.

AFM Characterization of Films

The topography of the prepared films was characterized by AFM measurements. This property is known to substantially affect the bulk properties of a material. Figure 7 shows the AFM 3D profile of neat CMC and CMC@GOn nanocomposite films. The AFM images show that the surface of the neat CMC film is quite smooth with an average surface roughness of 16 nm, whereas the images of CMC@GOn show that the average roughness of nanocomposite films gradually increases with the increasing of GOn loadings, showing a maximum of 59 nm for high GOn loading (7 wt %). This behavior was also previously observed for polymer nanocomposite films based on graphene and clay.[55,56] The relatively low values of average roughness observed for CMC@GOn films may be due to the good homogenous dispersion of nanosheets within the CMC matrix; additionally, no large aggregates were formed in resulting films. By considering these low values of roughness, the as-prepared CMC@GOn films have a very high smooth surface, which is a required property for packaging applications in combination with superior flexibility and mechanical strength of the films.

Mechanical Properties

The GOn's large aspect ratio and its very high Young's modulus should have a significant reinforcement impact on the mechanical properties of the polymer. Dispersion–exfoliation and homogenous distribution of GOn, along with favorable interfacial interactions between GOn and the polymer matrix are key points needed to achieve polymer nanocomposite films with enhanced final properties.[1,4]

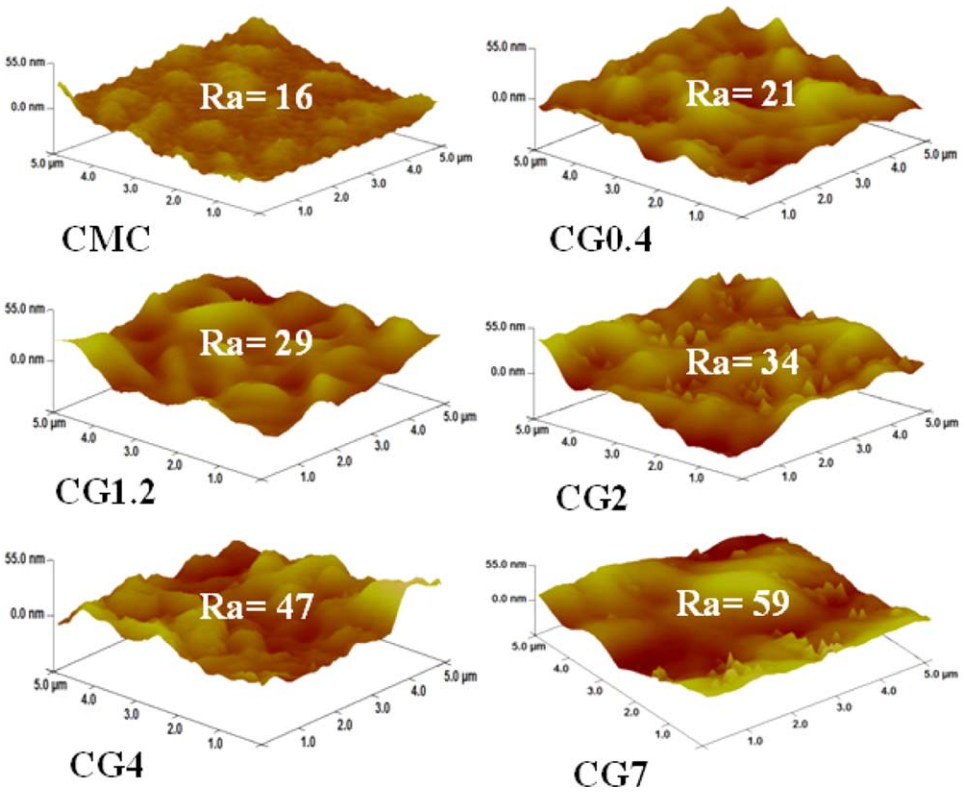

Figure 7. AFM 3D images showing surface features of neat CMC and CMC@GOn films with various GOn contents. *Ra* is the average toughness measured for each sample in *nm*. [Color figure can be viewed in the online issue, which is available at wileyonlinelibrary.com.]

The tensile properties of neat CMC film and its nanocomposite films with different GOn loadings were investigated by uni-axial tensile testing. Figure 8(a) shows the typical stress–strain curves of all the studied films. From these curves, the Young's modulus (E), the ultimate tensile strength (σ_s), the elongation at break (ε_b), and the toughness (T) were extracted and presented as a function of GOn contents in Figure 8(b–e). The cast neat CMC film shows a Young's modulus of 1.14 GPa, an ultimate tensile stress of 87.89 MPa, an elongation at break of 25.18% and a toughness of 16.96×10^{-6} J/m^3. These obtained values are the characteristics of a high molecular-weight CMC biopolymer.[26]

The addition of GOn gradually improved the selected tensile properties of the CMC matrix, for both low and high GOn loadings (0.4–7 wt %). The nanocomposite films containing only 0.4 wt % GOn (CG0.4 film) showed better mechanical properties with respect to the neat CMC film. The Young's modulus and the ultimate tensile strength of this nanocomposite film (CG0.4 film) were increased, respectively, by 51.75 and 44.60% with respect to the neat CMC film [Figure 8(b,c)]. When 1.2 wt % GOn is added (CG1.2 film), an increase of 166 and 107% for Young's modulus and tensile strength is achieved, respectively. Indeed, for low GOn loading ($\leq$1 wt %), our results are in agreement with previously reported results. Layek *et al.* studied GOn filled CMC nanocomposites with a maximum GOn loading of 1 wt %. For this GOn content, they observed that the Young's modulus and the tensile strength were increased by 154 and 188%, respectively; and this improvement was attributed to the hydrogen bonding interaction between GOn and CMC.[26] In the same way, Yadav *et al.* developed also GOn filled CMC nanocomposite at different GOn contents (0.5–1 wt %). A maximum increase of Young's modulus and tensile strength of 148 and 67% has been observed in the nanocomposite containing 1 wt % GOn.[27] Similar trends have been also observed for low GOn loading filled various commercial biopolymer matrices such as starch,[28] alginate,[29] polylactic acid,[30,31] and gelatin.[32]

For high GOn loading (up to 7 wt %), when very high improvement is needed, there are some previous reports regarding biopolymer based nanocomposite films.[57,58] It has been reported that the GOn start to aggregate when their loading level became higher than 3 wt %.[33–35] This can be attributed to the insufficient compatibility between the sheet and the polymer chains, leading to the sheet–sheet interaction. In this sense, Xu *et al.* studied the tensile properties of GOn-reinforced PVA nanocomposite films. It was found that the addition of 3 wt % GOn into PVA matrix resulted in the increase of Young's modulus and tensile strength by 128 and 70% in comparison with neat PVA polymer, but when 4 or 5 wt % of GOn was added, the nanocomposite films showed brittle failure, because the selected properties start to decrease in comparison with nanocomposite containing 3 wt % GOn, which was explained by the fact that the nanosheets start to aggregate when GOn loading became higher that 3 wt %.[33] Similarly, Jose *et al.* observed that the GOn nanosheets start to aggregate at 1 wt % GOn in PVA/starch blend matrix and the maximum increase of mechanical properties is observed for 0.5 wt % GOn.[34] The phenomenon of

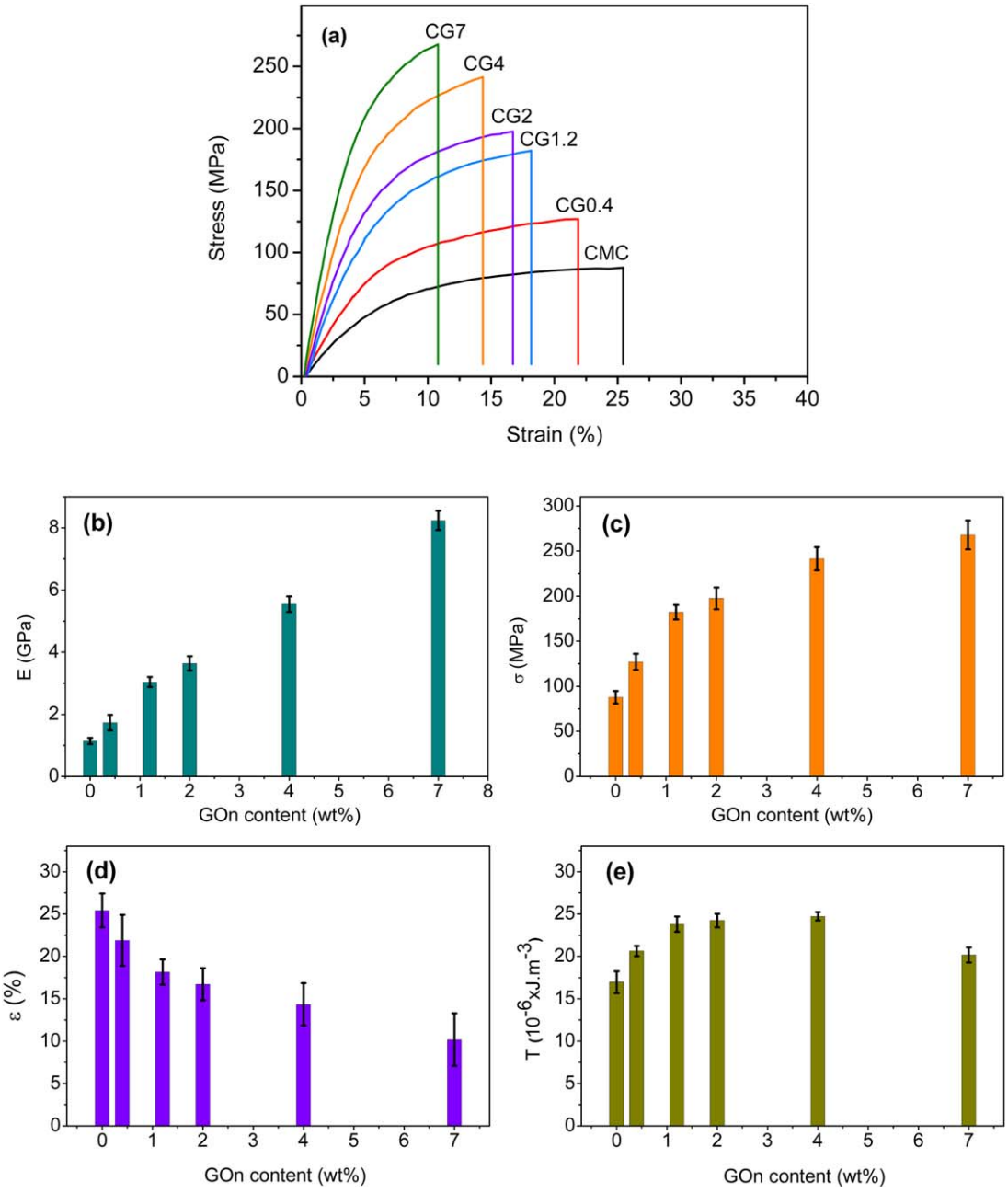

Figure 8. (**a**) Typical stress–strain curves of neat CMC and CMC@GOn films, (**b**) Plot of Young's modulus (E), (**c**) tensile strength (σ), (**d**) elongation at break (ε), and (**e**) toughness (T) as function of GOn content. [Color figure can be viewed in the online issue, which is available at wileyonlinelibrary.com.]

sheet aggregation is also observed by Zhang *et al.* in GOn/polyurethane nanocomposites, where the tensile properties of such nanocomposites start to decrease when more than 0.4 wt % GOn was added.[35]

From our results, the Young's modulus and the ultimate tensile strength were continuously improved up to 7 wt % GOn content, which were increased, respectively, by 623 (8.24 GPa) and 205% (267.77 MPa) for CG7 film with respect to the neat CMC. Herein, it is assumed that as the content of GOn increases, the phenomenon of nanosheets restacking together does not occur and the nanosheets are still well dispersed and distributed within the matrix; as evidenced by TEM observations (Figure 5). For highly filled biopolymers with GOn, some interesting results have been also reported. Pandele *et al.* measured the Young's modulus of GOn filled PVA/Chitosan blend. They observed that the modulus was gradually increased when GOn loading increase from 0.5 to 6 wt %. Which was ascribed to the strong interaction between GOn and PVA/Chitosan matrix, resulting in the good dispersion of GOn within the polymer matrix, which leads to a more uniform stress distribution and minimizes the presence of the stress concentration centers.[57] Han *et al.* prepared highly filled nanocomposite films based on GOn and chitosan by varying the GOn contents from

6 to 18 wt %. From their results, the tensile strength is gradually increased with increasing of GOn contents, and no aggregation of sheets has been observed, ascribing this finding to the molecule-level dispersion of GOn and the strong hydrogen bonding between the chitosan and the surface of GOn.[58] Therefore, the successful addition of high GOn content into biopolymer matrix strongly depends on the good compatibility and the strong interfacial interaction between the two phases. Herein, it was demonstrated that a high GOn content can be incorporated into CMC biopolymer without nanosheets aggregation, resulting in large improvement of mechanical properties of CMC@GOn nanocomposite films.

Besides, for comparing the reinforcement efficiency of GOn at high loading level with other nanofillers, we based on some reported works for CMC based nanocomposites. It has been reported that the addition of montmorillonite (MMT) into CMC increase gradually the Young's modulus and the tensile strength, with a maximum increase of 122 and 54% has been observed for the nanocomposite containing 10 wt % MMT, respectively.[59] Additionally, the dispersion of layered double hydroxide (LDH) into CMC biopolymer with LDH contents of 0–8 wt % was also reported. The maximum increase of Young's modulus (143%) and tensile strength (148%) has been observed for the 3 wt % LDH content. While these properties start to decrease when LDH content is higher than 3 wt %, which can be related to aggregation phenomenon.[37] Similarly, cellulose nanocrystals (CNC) have been also dispersed into CMC matrix by varying their contents from 5 to 30 wt %. However, the content of 5 wt % was the better for enhancing the mechanical properties, for which the Young's modulus and tensile strength were increased, respectively, by 85 and 30%.[60] Consequently, it is clear that the reinforcement efficiency of GOn, at high loading level, is large superior than other nanofillers for the development of CMC based nanocomposite materials.

More importantly, the large improvement of Young's modulus and tensile strength of CMC@GOn nanocomposites was accompanied by an increase of the toughness up to its maximum value of 24.74 $\times$ 106 J/m^3 for CMC@GOn nanocomposite films containing 4 wt % [Figure 8(e)]. Figure 8(d) shows that the elongation at break of the CMC@GOn films gradually decreases with GOn loading. The value of the elongation at break decreases to 10.18% for the nanocomposite with 7 wt % GOn loading (CG7). The reason may be attributed to the large aspect ratio and the strong interactions between GOn and the CMC matrix, which restricts the movement of the polymer chains. This trend is also observed in a variety of previously reported GOn filled biopolymer nanocomposite.[2,25–29]

Such improvement in mechanical properties of as-prepared CMC@GOn nanocomposite films was due to the presence of strong hydrogen-bonding interactions between CMC chains and GOn and the high nanodispersibility of GOn at the individual nanosheet level, even at high GOn content, which was related to the high compatibility between the two phases. These components were required to improve interfacial stress transfer from the polymer matrix to the individual nanosheets, thus increasing nanocomposite stiffness and mechanical properties. And it can be expected that CMC nanocomposites with largely improved mechanical properties may play a more important role in biomaterials or packaging materials applications. It is suggested that films suitable for food packaging should preferably be strong and flexible.[47] This trend was observed for the GOn filled CMC bionanocomposite films fabricated in the present work.

CONCLUSIONS

Mechanically strong and flexible nanocomposite films were prepared by dispersing exfoliated GOn into CMC biopolymer at low and high GOn contents (0.4, 1.2, 2, 4, and 7 wt %). An interconnected structure is assumed to be formed in CMC strengthened by GOn. The GOn's special 2D morphology and its functionalized surface allow obtaining a good homogeneous dispersion, which leads to a high contact area within the CMC matrix, for all GOn contents. This was mainly the result of a strong interaction between the macromolecular chains of CMC and the nanosheets of GOn. Due to these strong interfacial interactions, gradual improvements of structural, thermal, and mechanical properties has been obtained for GOn filled CMC nanocomposite films, for both low and high GOn contents. With the incorporation of 7 wt % GOn, 18% increase of thermal stability, 17% of glass transition temperature, 623% of Young's modulus, and 205% of tensile strength were achieved. This work produced high performances CMC-based nanocomposite films containing low and high loadings of well-dispersed GOn. Such nanocomposite films can be expected to have potential in biomaterials or packaging materials applications.

ACKNOWLEDGMENTS

The financial assistance of the Office Chérifien des Phosphates (OCP Group) in the Moroccan Kingdom toward this research is hereby acknowledged. This work was supported also by grant from the OCP Foundation. This work was performed as part of a collaboration between the Mohammed VI Polytechnic University and INRA-Montpellier. Financial support of the INRA-Montpellier is acknowledged. We equally thank all administrative and technical support teams of the *Université Mohammed VI Polytechnique*, especially Mrs Zoulikha EL BARKAOUI and Mrs Salima BALAFREJ.

REFERENCES

1. Rodríguez-González, C.; Martínez-Hernández, A. L.; Castaño, V. M.; Kharissova, O. V.; Ruoff, R. S.; Velasco-Santos, C. *Ind. Eng. Chem. Res.* **2012**, *51*, 3619.
2. Yang, X.; Tu, Y.; Li, L.; Shang, S.; Tao, X. *Appl. Mater. Int.* **2010**, *2*, 1707.
3. Goffin, A. L.; Raquez, J. M.; Duquesne, E.; Siqueira, G.; Habibi, Y.; Dufresne, A.; Dubois, P. *Biomacromolecules* **2011**, *12*, 2456.
4. Mittal, V. *Macromol. Mater. Eng.* **2014**, *299*, 906.
5. Sanchez-Garcia, M. D.; Lagaron, J. M.; Hoa, S. V. *Compos. Sci. Technol.* **2010**, *70*, 1095.
6. El Achaby, M.; Arrakhiz, F.-E.; Vaudreuil, S.; Essassi, E.; Qaiss, A.; Bousmina, M. *Polym. Eng. Sci.* **2013**, *53*, 34.
7. Schiffman, J. D.; Blackford, A. C.; Wegst, U. G. K.; Schauer, C. L. *Carbohydr. Polym.* **2011**, *84*, 1252.

8. Zhang, Q.; Mochalin, V. N.; Neitzel, I.; Hazeli, K.; Niu, J.; Kontsos, A.; Zhou, J. G.; Lelkes, P. I.; Gogotsi, Y. *Biomaterials* **2012**, *33*, 5067.
9. Balakrishnan, H.; Hassan, A.; Wahit, M. U.; Yussuf, A. A.; Razak, S. B. A. *Mater. Design* **2010**, *31*, 3289.
10. Camarero-Espinosa, S.; Boday, D. J.; Weder, C.; Foster, E. J. *J. Appl. Polym. Sci.* **2015**, *132*, 41607.
11. Novoselov, K. S.; Geim, A. K.; Morozov, S. V.; Jiang, D.; Zhang, Y.; Dubonos, S. V.; Grigorieva, I. V.; Firsov, A. A. *Science* **2004**, *306*, 666.
12. Ahmadi-Moghadam, B.; Sharafimasooleh, M.; Shadlou, S.; Taheri, F. *Mater. Design* **2015**, *66*, 142.
13. El Achaby, M.; Qaiss, A. *Mater. Design* **2013**, *44*, 81.
14. El Achaby, M.; Arrakhiz, F. E.; Vaudreuil, S.; Qaiss, A.; Bousmina, M.; Fassi-Fehri, O. *Polym. Compos.* **2012**, *33*, 733.
15. El Achaby, M.; Arrakhiz, F. E.; Vaudreuil, S.; Essassi, E.; Qaiss, A.; Bousmina, M. *J. Appl. Polym. Sci.* **2013**, *127*, 4697.
16. Dikin, D. A.; Stankovich, S.; Zimney, E. J.; Piner, R. D.; Dommett, G. H. B.; Evmenenko, G.; Nguyen, S. T.; Ruoff, R. S. *Nature* **2007**, *448*, 457.
17. Szabo, T.; Berkesi, O.; Forgo, P.; Josepovits, K.; Sanakis, Y.; Petridis, D.; Dekany, I. *Chem. Mater.* **2006**, *18*, 2740.
18. Acik, M.; Mattevi, C.; Gong, C.; Lee, G.; Cho, K.; Chhowalla, M.; Chabal, Y. J. *ACS Nano* **2010**, *4*, 5861.
19. Stankovich, S.; Dikin, D. A.; Piner, R. D.; Kohlhaas, K. A.; Kleinhammes, A.; Jia, Y.; Wu, Y.; Nguyen, S. T.; Ruoff, R. S. *Carbon* **2007**, *45*, 1558.
20. Eda, G.; Fanchini, G.; Chhowalla, M. *Nat. Nanotechnol.* **2008**, *3*, 270.
21. Robinson, J. T.; Zalalutdinov, M.; Baldwin, J. W.; Snow, E. S.; Wei, Z.; Sheehan, P.; Houston, B. H. *Nano Lett.* **2008**, *8*, 3441.
22. Liu, Z.; Robinson, J. T.; Sun, X.; Dai, H. *J. Am. Chem. Soc.* **2008**, *130*, 10876.
23. Tylianakis, E.; Psofogiannakis, G. M.; Froudakis, G. E. *J. Phys. Chem. Lett.* **2010**, *1*, 2459.
24. Ng, Y. H.; Iwase, A.; Kudo, A.; Amal, R. *J. Phys. Chem. Lett.* **2010**, *1*, 2607.
25. Han, D.; Yan, L.; Chen, W.; Li, W. *Carbohydr. Polym.* **2011**, *83*, 653.
26. Layek, R. K.; Kundu, A.; Nandi, A. K. *Macromol. Mater. Eng.* **2013**, *298*, 1166.
27. Yadav, M.; Rhee, K. Y.; Jung, I. H.; Park, S. J. *Cellulose* **2013**, *20*, 687.
28. Li, R.; Liu, C.; Ma, J. *Carbohydr. Polym.* **2011**, *84*, 631.
29. Ionita, M.; Pandele, M. A.; Iovu, H. *Carbohydr. Polym.* **2013**, *94*, 339.
30. Shen, Y.; Jing, T.; Ren, W.; Zhang, J.; Jiang, Z. G.; Yu, Z. Z.; Dasari, A. *Compos. Sci. Technol.* **2012**, *72*, 1430.
31. Li, W.; Xu, Z.; Chen, L.; Shan, M.; Tian, X.; Yang, C.; Lv, H.; Qian, X. *Chem. Eng. J.* **2014**, *237*, 291.
32. Wang, C.; Frydrych, M.; Chen, B. *Soft Matter* **2011**, *7*, 6159.
33. Xu, Y.; Hong, W.; Bai, H.; Li, C.; Shi, G. *Carbon* **2009**, *47*, 3538.
34. Jose, J.; Al-Harthi, M. A.; AlMa'adeed, M. A.; Dakua, J. B.; De, S. K. *J. Appl. Polym. Sci.* **2015**, *132*, 41827.
35. Zhang, J.; Zhang, C.; Madbouly, S. A. *J. Appl. Polym. Sci.* **2015**, *132*, 41751.
36. Grzadka, E.; Chibowski, S. *Cellulose* **2012**, *19*, 23.
37. Yadollahi, M.; Namazi, H.; Barkhordari, S. *Carbohydr. Polym.* **2014**, *108*, 83.
38. Gayrish, G. A.; Saychenko, N.; Kozlova, Y.; Melanichenko, I. V.; Liptuga, N. I. U.S. Pat. 87,429,3505; **1989**.
39. Zhang, Y.; Liu, Y.; Wang, X.; Sun, Z.; Ma, J.; Wu, T.; Xing, F.; Gao, J. *Carbohydr. Polym.* **2014**, *101*, 392.
40. Kniewske, R.; Kiesewetter, R.; Reinhardt, E.; Szablikowski, K. D.E. Pat. 92,423,9553; **1994**.
41. Lee, M. U.S. Pat. 50,892,66; **1992**.
42. Leupin, J. A.; Gosselink, E. P. W.O. Pat. 99,142,95; **1999**.
43. Seiichi, I.; Shosuke, W. J.P. Pat. 98,186,280; **2000**.
44. Khan, R. A.; Salmieri, S.; Dussault, D.; Uribe-Calderon, J.; Kamal, M. R.; Safrany, A.; Lacroix, M. *J. Agric. Food Chem.* **2010**, *58*, 7878.
45. Wang, J.; Feng, M.; Zhan, H. *Opt. Laser Technol.* **2014**, *57*, 84.
46. El Achaby, M.; Arrakhiz, F. E.; Vaudreuil, S.; Essassi, E.; Qaiss, A. *Appl. Surf. Sci.* **2012**, *258*, 7668.
47. El Achaby, M.; Essamlali, Y.; El Miri, N.; Snik, A.; Abdelouahdi, K.; Fihri, A.; Zahouily, M.; Solhy, A. *J. Appl. Polym. Sci.* **2014**, *131*, 41042.
48. Parades, J. I.; Villar-Rodil, S.; Martinez-Alonso, A.; Tascon, J. M. D. *Langmuir* **2008**, *24*, 10560.
49. Wu, D.; Wang, J.; Zhang, M.; Zhou, W. *Ind. Eng. Chem. Res.* **2012**, *51*, 6705.
50. El Miri, N.; Abdelouahdi, K.; Zahouily, M.; Fihri, A.; Barakat, A.; Solhy, A.; El Achaby, M. *J. Appl. Polym. Sci.* **2015**, *132*, 42004.
51. Luna-Martínez, J. F.; Hernández-Uresti, D. B.; Reyes-Melo, M. E.; Guerrero-Salazara, C. A.; González-González, V. A.; Sepúlveda-Guzmán, S. *Carbohydr. Polym.* **2011**, *84*, 566.
52. Bagri, A.; Mattevi, C.; Acik, M.; Chabal, Y. J.; Chhowalla, M.; Shenoy, V. B. *Nat. Chem.* **2010**, *2*, 581.
53. Levi, N.; Czerw, R.; Xing, S.; Iyer, P.; Carroll, D. L. *Nano Lett.* **2004**, *4*, 1267.
54. Manna, S.; Nandi, A. K. *J. Phys. Chem. C* **2007**, *111*, 14670.
55. Longun, J.; Walker, G.; Iroh, J. O. *Carbon* **2013**, *63*, 9.
56. Gaume, J.; Taviot-Gueho, C.; Cros, S.; Rivaton, A.; Thérias, S.; Gardette, J. L. *Sol. Energy Mater. Sol. Cells* **2012**, *99*, 240.
57. Pandele, A. M.; Ionita, M.; Crica, L.; Dinescu, S.; Costache, M.; Iovu, H. *Carbohydr. Polym.* **2014**, *102*, 813.
58. Han, D.; Yan, L.; Chen, W.; Li, W. *Carbohydr. Polym.* **2011**, *83*, 653.
59. Gutiérrez, M. Q.; Echeverría, I.; Ihl, M.; Bifani, V.; Maur, A. N. *Carbohydr. Polym.* **2012**, *87*, 1495.
60. Choi, Y.; Simonsen, J. *J. Nanosci. Nanotechnol.* **2006**, *6*, 633.